Energy-preserving Variational Integrators for Forced Lagrangian Systems

Harsh Sharma [*,†], Mayuresh Patil [‡], and Craig Woolsey [§]
Virginia Polytechnic Institute and State University, Blacksburg, VA, 24061

July 25, 2019

Abstract

The goal of this paper is to develop energy-preserving variational integrators for time-dependent mechanical systems with forcing. We first present the Lagrange-d'Alembert principle in the extended Lagrangian mechanics framework and derive the extended forced Euler-Lagrange equations in continuous-time. We then obtain the extended forced discrete Euler-Lagrange equations using the extended discrete mechanics framework and derive adaptive time step variational integrators for time-dependent Lagrangian systems with forcing. We consider three numerical examples to study the numerical performance of energy-preserving variational integrators. First, we consider the example of a nonlinear conservative system to illustrate the advantages of using adaptive time-stepping in variational integrators. In addition, we demonstrate how the implicit equations become more ill-conditioned as the adaptive time step decreases through a condition number analysis. As a second example, we numerically simulate the time-dependent example of a forced harmonic oscillator to demonstrate the superior energy performance of energy-preserving integrators for mechanical systems with explicit time-dependent forcing. Finally, we consider a damped harmonic oscillator using the adaptive time step variational integrator framework. The adaptive time step increases monotonically for the dissipative system leading to unexpected energy behavior. Modified abstract.

Keywords: Energy-preserving integrators; Variational integrators; Adaptive time-step integrators; Discrete mechanics.

1 Introduction

In engineering applications, numerical integrators for equations of motion are usually derived by discretizing differential equations. These traditional integrators do not account for the inherent geometric structure of the governing continuous-time equations, which results in numerical methods that introduce numerical dissipation and do not preserve invariants of the system. The field of geometric numerical integration is concerned with numerical methods that preserve the structure of the problem and the corresponding geometric properties of the differential equations. A brief introduction to the field of geometric numerical integration can be found in [1] and various techniques for constructing structure-preserving integrators for ordinary differential equations are given in [2] .

Ge and Marsden [3] showed that a fixed time step numerical integrator cannot preserve the symplectic form, momentum, and energy simultaneously for non-integrable systems. Based on this result, structure-preserving fixed time step mechanical integrators can be divided into two categories, symplectic-momentum, and energy-momentum integrators. Even though symplectic-momentum integrators do not conserve energy exactly, they have been shown to exhibit good long-time energy behavior. On the other hand, Simo and his collaborators [4, 5] have developed mechanical integrators that conserve energy and momentum but do not preserve the symplectic form.

[*]Corresponding Author, Email Address for Correspondence: harshs3@vt.edu
[†]Ph.D. Candidate, Kevin T. Crofton Department of Aerospace and Ocean Engineering
[‡]Associate Professor, Kevin T. Crofton Department of Aerospace and Ocean Engineering
[§]Professor, Kevin T. Crofton Department of Aerospace and Ocean Engineering

Variational integrators are a class of structure-preserving integrators, that are derived by discretizing the action principle rather than the governing differential equation. The basic idea behind these methods is to obtain an approximation of the action integral called the discrete action. Stationary points of the discrete action give discrete time trajectories of the mechanical system. These integrators have good long-time energy behavior and they conserve the invariants of the dynamics in the presence of symmetries. The basics of variational integrators can be reviewed in [6] and more detailed theory can be found in [7]. A more general framework encompassing variational integrators, asynchronous variational integrators, and symplectic-energy-momentum integrators is discussed in [8]. Due to their symplectic nature, variational integrators are ideal for long-time simulation of conservative or weakly dissipative systems found in astrophysics and molecular dynamics. The discrete trajectories obtained using variational integrators display excellent energy behavior for exponentially long times.

The fixed time step variational integrators derived from the discrete variational principle cannot preserve the energy of the system exactly. To conserve the energy in addition to preserving the symplectic structure and conserving the momentum, time adaptation needs to be used. These symplectic-energy-momentum integrators were first developed for conservative systems in [9] by imposing an additional energy preservation equation to compute the time step. The same integrators were derived through a variational approach for a more general case of time-dependent Lagrangian systems in [7] by preserving the discrete energy obtained from the discrete variational principle in the extended phase space.

Numerically equivalent methods were derived independently through the Hamiltonian approach by Shibberu in [10]. Shibberu has discussed the well-posedness of symplectic-energy-momentum integrators in [11] and suggested ways to regularize the governing set of nonlinear discrete equations in [12]. These symplectic-energy-momentum integrators require solving a coupled nonlinear implicit system of equations at every time step to update the configuration variables and time variable. The time-marching equations for these energy-preserving integrators are ill-conditioned for arbitrarily small time steps and existence of solutions for these discrete trajectories is still an open problem.

The purpose of this paper is twofold. First, we develop variational integrators for time-dependent Lagrangian systems with nonconservative forces based on the discretization of the Lagrange-d'Alembert principle in extended phase space. We modify the Lagrange-d'Alembert principle to include time variations in the extended phase space and derive the extended forced Euler-Lagrange equations. We then present a discrete variational principle for time-dependent Lagrangian systems with forcing and derive extended forced discrete Euler-Lagrange equations. We use the extended discrete mechanics formulation to construct adaptive time step variational integrators for nonautonomous Lagrangian systems with forcing that capture the rate of energy evolution accurately. Second, we consider three numerical examples to understand the numerical properties of the adaptive time step variational integrators and compare the results with fixed time step variational integrators to illustrate the advantages of using adaptive time-stepping in variational integrators. We also study the effect of initial time step and initial conditions on the numerical performance of the adaptive time step variational integrators.

The remainder of the paper is organized as follows. In Section 2, we review the basics of extended Lagrangian mechanics and discrete mechanics. We also discretize Hamilton's principle to derive adaptive time step variational integrators. In Section 3, we modify the Lagrange-d'Alembert principle in the extended phase space and derive extended forced Euler-Lagrange equations. In Section 4, we derive the extended forced discrete Euler-Lagrange equations and obtain adaptive time step variational integrators for time-dependent Lagrangian systems with forcing. In Section 5, we give numerical examples to understand the numerical performance of the adaptive time step variational integrators. Finally, in Section 6 we provide concluding remarks and suggest future research directions.

2 Background: Adaptive Time Step Variational Integrators

Shortened this section to 2 pages after the comment by second reviewer In this section, we review the basics of Lagrangian mechanics and derivation of adaptive time step variational integrators. Drawing on the work of Marsden et al. [9, 13, 7], we first derive equations of motion in continuous-time from the variational principle and then derive variational integrators by considering the discretized variational principle in the discrete-time domain. To this end, we first derive continuous-time Euler-Lagrange equations of motion from Hamilton's principle. After deriving

equations of motion, we use concepts of discrete mechanics developed in [7] to derive discrete Euler-Lagrange equations and then write them in the time-marching form to obtain adaptive time step variational integrators for Lagrangian systems.

2.1 Extended Lagrangian Mechanics

Hamilton's principle of stationary action is one of the most fundamental results of classical mechanics and is commonly used to derive equations of motion for a variety of systems. The forces and interactions that govern the dynamical evolution of the system are easily determined through Hamilton's principle in a formulaic and elegant manner. Hamilton's principle [14] states that: The motion of the system between two fixed points from t_i to t_f is such that the action integral has a stationary value for the actual path of the motion. In order to derive the Euler-Lagrange equations via Hamilton's principle, we start by defining the configuration space, tangent space and path space.

Consider a time-dependent Lagrangian system with configuration manifold Q and time space $\mathbb{R}$. In the extended Lagrangian mechanics framework [7], we treat time as a dynamic variable and define the extended configuration manifold $\bar{Q} = \mathbb{R} \times Q$; the corresponding state space $T\bar{Q}$ is $\mathbb{R} \times TQ$. The extended Lagrangian is $L : \mathbb{R} \times TQ \to \mathbb{R}$.

In the extended Lagrangian mechanics framework, t and $\mathbf{q}$ are both parametrized by an independent variable a. The two components of a trajectory c are $c(a) = (c_t(a), c_{\mathbf{q}}(a))$. The extended path space is

$$\bar{\mathcal{C}} = \left\{ c : [a_0, a_f] \to \bar{Q} |\ c \textit{ is a } C^2 \textit{ curve and } c_t'(a) > 0 \right\} \tag{1}$$

For a given path $c(a)$, the initial time is $t_0 = c_t(a_0)$ and the final time is $t_f = c_t(a_f)$. The extended action $\bar{\mathfrak{B}} : \bar{\mathcal{C}} \to \mathbb{R}$ is

$$\bar{\mathfrak{B}} = \int_{t_0}^{t_f} L(t, \mathbf{q}(t), \dot{\mathbf{q}}(t)) dt \tag{2}$$

Since time is a dynamic variable in this framework, we substitute $(t, \mathbf{q}(t), \dot{\mathbf{q}}(t)) = \left(c_t(a), c_{\mathbf{q}}(a), \frac{c_{\mathbf{q}}'(a)}{c_t'(a)} \right)$ in the above equation to get

$$\bar{\mathfrak{B}} = \int_{a_0}^{a_f} L\left(c_t(a), c_q(a), \frac{c_q'(a)}{c_t'(a)} \right) c_t'(a)\ da \tag{3}$$

We compute variations of the action

$$\delta\bar{\mathfrak{B}} = \int_{a_0}^{a_f} \left[\frac{\partial L}{\partial t}\delta c_t + \frac{\partial L}{\partial \mathbf{q}} \cdot \delta c_{\mathbf{q}} + \frac{\partial L}{\partial \dot{\mathbf{q}}} \cdot \left(\frac{\delta c_{\mathbf{q}}'(a)}{c_t'} - \frac{c_{\mathbf{q}}' \delta c_t'(a)}{(c_t')^2} \right) \right] c_t'(a) da + \int_{a_0}^{a_f} L \delta c_t'(a)\ da \tag{4}$$

Using integration by parts and setting the variations at the end points to zero gives

$$\delta\bar{\mathfrak{B}} = \int_{a_0}^{a_f} \left[\frac{\partial L}{\partial \mathbf{q}} c_t' - \frac{d}{da}\frac{\partial L}{\partial \dot{\mathbf{q}}} \right] \cdot \delta c_{\mathbf{q}}(a) da + \int_{a_0}^{a_f} \left[\frac{\partial L}{\partial t} c_t' + \frac{d}{da}\left(\frac{\partial L}{\partial \dot{\mathbf{q}}} \cdot \frac{c_{\mathbf{q}}'}{c_t'} - L \right) \right] \delta c_t(a)\ da \tag{5}$$

Using $dt = c_t'(a)da$ in the above expression gives two equations of motion. The first is the Euler-Lagrange equation of motion

$$\frac{\partial L}{\partial \mathbf{q}} - \frac{d}{dt}\left(\frac{\partial L}{\partial \dot{\mathbf{q}}} \right) = \mathbf{0} \tag{6}$$

which is the same as the equation obtained using the classical Lagrangian mechanics framework. The second equation is

$$\frac{\partial L}{\partial t} + \frac{d}{dt}\left(\frac{\partial L}{\partial \dot{\mathbf{q}}} \cdot \dot{\mathbf{q}} - L \right) = 0 \tag{7}$$

which describes how the energy of the system evolves with time.

2.2 Energy-preserving Variational Integrators

For the extended Lagrangian mechanics, we define the extended discrete state space $\bar{Q} \times \bar{Q}$. The extended discrete path space is

$$\bar{\mathcal{C}}_d = \{\ c : \{\ 0, ..., N\} \to \bar{Q} |\ \ c_t(k+1) > c_t(k)\ \ \textit{for all } k\} \tag{8}$$

The extended discrete action map $\bar{\mathcal{B}}_d : \bar{\mathcal{C}}_d \to \mathbb{R}$ is

$$\bar{\mathcal{B}}_d = \sum_{k=0}^{N-1} L_d(t_k, \mathbf{q}_k, t_{k+1}, \mathbf{q}_{k+1}) \tag{9}$$

where $L_d : \bar{Q} \times \bar{Q} \to \mathbb{R}$ is the extended discrete Lagrangian function which approximates the action integral between two successive configurations. Taking variations of the extended discrete action map gives

$$\begin{aligned}\delta \bar{B}_d = \sum_{k=1}^{N-1} \left[D_4 L_d(t_{k-1}, \mathbf{q}_{k-1}, t_k, \mathbf{q}_k) + D_2 L_d(t_k, \mathbf{q}_k, t_{k+1}, \mathbf{q}_{k+1}) \right] \cdot \delta \mathbf{q}_k \\ + \sum_{k=1}^{N-1} \left[D_3 L_d(t_{k-1}, \mathbf{q}_{k-1}, t_k, \mathbf{q}_k) + D_1 L_d(t_k, \mathbf{q}_k, t_{k+1}, \mathbf{q}_{k+1}) \right] \delta t_k = 0\end{aligned} \tag{10}$$

where D_i denotes differentiation with respect to the i^{th} argument of the discrete Lagrangian L_d. Applying Hamilton's principle of least action and setting variations at end points to zero gives the extended discrete Euler-Lagrange equations

$$D_4 L_d(t_{k-1}, \mathbf{q}_{k-1}, t_k, \mathbf{q}_k) + D_2 L_d(t_k, \mathbf{q}_k, t_{k+1}, \mathbf{q}_{k+1}) = \mathbf{0} \tag{11}$$

$$D_3 L_d(t_{k-1}, \mathbf{q}_{k-1}, t_k, \mathbf{q}_k) + D_1 L_d(t_k, \mathbf{q}_k, t_{k+1}, \mathbf{q}_{k+1}) = 0 \tag{12}$$

Given $(t_{k-1}, \mathbf{q}_{k-1}, t_k, \mathbf{q}_k)$, the extended discrete Euler-Lagrange equations can be solved to obtain $\mathbf{q}_{k+1}$ and t_{k+1}. This extended discrete Lagrangian system can be seen as a numerical integrator of the continuous-time nonautonomous Lagrangrian system with adaptive time steps.

In the extended discrete mechanics framework, we define the discrete momentum $\mathbf{p}_k$ by

$$\mathbf{p}_k = D_4 L_d(t_{k-1}, \mathbf{q}_{k-1}, t_k, \mathbf{q}_k) \tag{13}$$

We also introduce the discrete energy

$$E_k = D_3 L_d(t_{k-1}, \mathbf{q}_{k-1}, t_k, \mathbf{q}_k) \tag{14}$$

Using the discrete momentum and discrete energy definitions, we can re-write the extended discrete Euler-Lagrange equations (11) and (12) in the following form

$$-D_2 L_d(t_k, \mathbf{q}_k, t_{k+1}, \mathbf{q}_{k+1}) = \mathbf{p}_k \tag{15}$$

$$D_1 L_d(t_k, \mathbf{q}_k, t_{k+1}, \mathbf{q}_{k+1}) = E_k \tag{16}$$

$$\mathbf{p}_{k+1} = D_4 L_d(t_k, \mathbf{q}_k, t_{k+1}, \mathbf{q}_{k+1}) \tag{17}$$

$$E_{k+1} = -D_3 L_d(t_k, \mathbf{q}_k, t_{k+1}, \mathbf{q}_{k+1}) \tag{18}$$

Given $(t_k, \mathbf{q}_k, \mathbf{p}_k, E_k)$, the coupled nonlinear equations (15) and (16) are solved implicitly to obtain $\mathbf{q}_{k+1}$ and t_{k+1}. The configuration $\mathbf{q}_{k+1}$ and time t_{k+1} are then used in (17) and (18) to obtain $(\mathbf{p}_{k+1}, E_{k+1})$ explicitly. The extended discrete Euler-Lagrange equations were first written in the time-marching form in [7] and are also known as symplectic-energy-momentum integrators.

3 Modified Lagrange-d'Alembert Principle

The extended discrete Euler-Lagrange equations derived in Section 2.2 can be used as energy-preserving variational integrators for Lagrangian systems. In order to extend this energy-preserving variational integrator framework to Lagrangian systems with external forcing, we need to discretize the Lagrange-d'Alembert principle in the extended Lagrangian mechanics framework. We first present the Lagrange- d'Alembert principle in extended phase space for time-dependent Lagrangian systems with forcing by considering the variations with respect to time t. Using the extended Lagrangian mechanics framework, we derive the extended Euler-Lagrange equations for time-dependent Lagrangian systems with forcing.

The Lagrange- d'Alembert principle modifies Hamilton's principle of stationary action by considering the virtual work done by the forces for a variation $\delta\mathbf{q}$ in the configuration variable $\mathbf{q}$. Since the standard Lagrangian mechanics framework treats time only as an independent continuous parameter, it does not account for time variations in the Lagrange-d'Alembert principle. Thus, we need to modify the Lagrange-d'Alembert principle in the extended Lagrangian mechanics framework to account for time variations.

We modify the Lagrange-d'Alembert principle by adding an additional term in the variational principle that accounts for virtual work done by the external force $\mathbf{f}_L$ due to variations in the time variable

$$\delta \int_{t_0}^{t_f} L(t, \mathbf{q}(t), \dot{\mathbf{q}}(t))\ dt + \int_{t_0}^{t_f} \mathbf{f}_L(t, \mathbf{q}(t), \dot{\mathbf{q}}(t)) \cdot \delta\mathbf{q}\ dt - \int_{t_0}^{t_f} \mathbf{f}_L(t, \mathbf{q}(t), \dot{\mathbf{q}}(t)) \cdot (\dot{\mathbf{q}}\delta t)\ \ dt = 0 \quad (19)$$

Using the extended Lagrangian mechanics framework discussed in Section 2.1 to derive the equations of motion, we first re-write the modified Lagrange-d'Alembert principle

$$\delta \int_{a_0}^{a_f} L\left(c_t(a), c_{\mathbf{q}}(a), \frac{c'_{\mathbf{q}}(a)}{c'_t(a)}\right) c'_t(a)\ da + \int_{a_0}^{a_f} f_L\left(c_t(a), c_{\mathbf{q}}(a), \frac{c'_{\mathbf{q}}(a)}{c'_t(a)}\right) \cdot (\delta c_{\mathbf{q}} - \dot{\mathbf{q}}\delta c_t)\ c't(a)da = 0 \quad (20)$$

Taking variations of the discrete action with respect to both configuration $\mathbf{q}$ and time t gives

$$\int_{a_0}^{a_f} \left[\frac{\partial L}{\partial t}\delta c_t + \frac{\partial L}{\partial \mathbf{q}} \cdot \delta c_{\mathbf{q}} + \frac{\partial L}{\partial \dot{\mathbf{q}}} \cdot \left(\frac{\delta c'_{\mathbf{q}}(a)}{c'_t} - \frac{c'_{\mathbf{q}}\delta c'_t(a)}{(c'_t)^2}\right)\right] c'_t(a)da + \int_{a_0}^{a_f} L\delta c'_t(a)\ da$$
$$+ \int_{a_0}^{a_f} (f_L \cdot \delta c_{\mathbf{q}})\ \ c't(a)da - \int_{a_0}^{a_f} (f_L \cdot \dot{\mathbf{q}})\, \delta c_t\ c't(a)da = 0 \quad (21)$$

Using integration by parts and setting variations at the end points to zero gives

$$\int_{a_0}^{a_f} \left[\frac{\partial L}{\partial \mathbf{q}}c'_t - \frac{d}{da}\frac{\partial L}{\partial \dot{\mathbf{q}}} + \mathbf{f}_L\right] \cdot \delta c_{\mathbf{q}}(a)da + \int_{a_0}^{a_f} \left[\frac{\partial L}{\partial t}c'_t + \frac{d}{da}\left(\frac{\partial L}{\partial \dot{\mathbf{q}}} \cdot \frac{c'_{\mathbf{q}}}{c'_t} - L\right) - \mathbf{f}_L \cdot \dot{\mathbf{q}}\right] \delta c_t(a)\ da = 0 \quad (22)$$

Using $dt = c'_t(a)da$ in the above expression gives two equations of motion for the forced time-dependent Lagrangian system. The first equation is the well-known forced Euler-Lagrange equation for a time-dependent system

$$\frac{\partial L}{\partial \mathbf{q}} - \frac{d}{dt}\left(\frac{\partial L}{\partial \dot{\mathbf{q}}}\right) + \mathbf{f}_L = \mathbf{0} \quad (23)$$

whereas the second equation is the energy evolution equation

$$\frac{\partial L}{\partial t} + \frac{d}{dt}\left(\frac{\partial L}{\partial \dot{\mathbf{q}}}\dot{\mathbf{q}} - L\right) - \mathbf{f}_L \cdot \dot{\mathbf{q}} = 0 \quad (24)$$

Thus, for the forced case, the energy evolution equation describes how the energy of the Lagrangian system depends on the input power by the external force $\mathbf{f}_L$. If we consider an associated curve $\mathbf{q}(t)$ satisfying the forced Euler-Lagrange equations and compute the energy evolution equation we get

$$\frac{\partial L}{\partial t} + \frac{d}{dt}\left(\frac{\partial L}{\partial \dot{\mathbf{q}}}.\dot{\mathbf{q}} - L\right) - \mathbf{f}_L.\dot{\mathbf{q}} = \frac{\partial L}{\partial t} + \frac{d}{dt}\left(\frac{\partial L}{\partial \dot{\mathbf{q}}}\right).\dot{\mathbf{q}} + \frac{\partial L}{\partial \dot{\mathbf{q}}}.\ddot{\mathbf{q}} - \frac{dL}{dt} - \mathbf{f}_L.\dot{\mathbf{q}} \quad (25)$$

which after substituting $\frac{d}{dt}\left(\frac{\partial L}{\partial \dot{\mathbf{q}}}\right) = \frac{\partial L}{\partial \mathbf{q}} + \mathbf{f}_L$ simplifies to

$$\frac{\partial L}{\partial t} + \frac{d}{dt}\left(\frac{\partial L}{\partial \dot{\mathbf{q}}}.\dot{\mathbf{q}} - L\right) - \mathbf{f}_L.\dot{\mathbf{q}} = \left(\frac{\partial L}{\partial t} + \left(\frac{\partial L}{\partial \mathbf{q}} + \mathbf{f}_L\right).\dot{\mathbf{q}} + \frac{\partial L}{\partial \dot{\mathbf{q}}}.\ddot{\mathbf{q}}\right) - \frac{dL}{dt} - \mathbf{f}_L.\dot{\mathbf{q}} = 0 \quad (26)$$

which shows that (23) implies (24). Thus, for continuous-time forced Lagrangian systems, the additional energy evolution equation obtained by taking the variation with respect to time does not provide any new information concerning the forced Euler-Lagrange equations.

Remark 1. It should be noted that both (23) and (24) depend only on the associated curve $\mathbf{q}(t)$ and the time component $c_t(a)$ of the extended path cannot be determined from the governing equations. Thus, the "velocity" of time, i.e. $c'_t(a)$, is indeterminate in the continuous-time formulation of time-dependent Lagrangian systems with forcing.

4 Energy-preserving Variational Integrators

In this section, we derive the extended discrete Euler-Lagrange equations for time-dependent Lagrangian systems with forcing by discretizing the modified Lagrange-d'Alembert principle given in Section 3. The key difference from the extended discrete Euler-Lagrange equations derived in Section 2.2 is that we will have additional discrete terms accounting for the virtual work done by the external forcing.

The modified Lagrange-d'Alembert principle presented in Section 3 has two continuous-time force integrals in the variational principle. In order to derive the extended forced discrete Euler-Lagrange equations, we define two discrete force terms $f_d^{\pm} : \bar{Q} \times \bar{Q} \to T^*\bar{Q}$ which approximate the virtual work done due to variations in $\mathbf{q}$ in the following sense

$$f_d^+(t_k, \mathbf{q}_k, t_{k+1}, \mathbf{q}_{k+1}) \cdot \delta\mathbf{q}_{k+1} + f_d^-(t_k, \mathbf{q}_k, t_{k+1}, \mathbf{q}_{k+1}) \cdot \delta\mathbf{q}_k \approx \int_{t_k}^{t_{k+1}} \mathbf{f}_L(t, \mathbf{q}(t), \dot{\mathbf{q}}(t)) \cdot \delta\mathbf{q} \; dt \quad (27)$$

We also define two discrete power terms $g_d^{\pm} : \bar{Q} \times \bar{Q} \to \mathbb{R}$ which approximate the virtual work done due to time variations in the following sense

$$g_d^+(t_k, \mathbf{q}_k, t_{k+1}, \mathbf{q}_{k+1})\delta t_{k+1} + g_d^-(t_k, \mathbf{q}_k, t_{k+1}, \mathbf{q}_{k+1})\delta t_k \approx \int_{t_k}^{t_{k+1}} -\mathbf{f}_L(t, \mathbf{q}(t), \dot{\mathbf{q}}(t)) \cdot (\dot{\mathbf{q}}\delta t) \; dt \quad (28)$$

For the time-dependent Lagrangian system with forcing, we seek discrete-time paths which satisfy

$$\begin{aligned}\delta \sum_{k=0}^{N-1} L_d(t_k, \mathbf{q}_k, t_{k+1}, \mathbf{q}_{k+1}) + \sum_{k=0}^{N-1} [\mathbf{f}_d^+(t_k, \mathbf{q}_k, t_{k+1}, \mathbf{q}_{k+1}) \cdot \delta\mathbf{q}_{k+1} + \mathbf{f}_d^-(t_k, \mathbf{q}_k, t_{k+1}, \mathbf{q}_{k+1}) \cdot \delta\mathbf{q}_k] \\ + \sum_{k=0}^{N-1} [g_d^+(t_k, \mathbf{q}_k, t_{k+1}, \mathbf{q}_{k+1})\delta t_{k+1} + g_d^-(t_k, \mathbf{q}_k, t_{k+1}, \mathbf{q}_{k+1})\delta t_k] = 0 \quad (29)\end{aligned}$$

Setting all the variations at the endpoints equal to zero in (29) gives the extended forced discrete Euler-Lagrange equations

$$D_4 L_d(t_{k-1}, \mathbf{q}_{k-1}, t_k, \mathbf{q}_k) + D_2 L_d(t_k, \mathbf{q}_k, t_{k+1}, \mathbf{q}_{k+1}) + \mathbf{f}_d^+(t_{k-1}, \mathbf{q}_{k-1}, t_k, \mathbf{q}_k) + \mathbf{f}_d^-(t_k, \mathbf{q}_k, t_{k+1}, \mathbf{q}_{k+1}) = \mathbf{0} \quad (30)$$

$$D_3 L_d(t_{k-1}, \mathbf{q}_{k-1}, t_k, \mathbf{q}_k) + D_1 L_d(t_k, \mathbf{q}_k, t_{k+1}, \mathbf{q}_{k+1}) + g_d^+(t_{k-1}, \mathbf{q}_{k-1}, t_k, \mathbf{q}_k) + g_d^-(t_k, \mathbf{q}_k, t_{k+1}, \mathbf{q}_{k+1}) = 0 \quad (31)$$

We modify the definitions of the discrete momentum and energy to account for the effect of forcing

$$\mathbf{p}_k = D_4 L_d(t_{k-1}, \mathbf{q}_{k-1}, t_k, \mathbf{q}_k) + \mathbf{f}_d^+(t_{k-1}, \mathbf{q}_{k-1}, t_k, \mathbf{q}_k) \quad (32)$$

$$E_k = -D_3 L_d(t_{k-1}, \mathbf{q}_{k-1}, t_k, \mathbf{q}_k) - g_d^+(t_{k-1}, \mathbf{q}_{k-1}, t_k, \mathbf{q}_k) \quad (33)$$

Using the modified discrete momentum and energy definitions (32) and (33), the extended forced discrete Euler-Lagrange equations can be re-written in the following form

$$-D_2 L_d(t_k, \mathbf{q}_k, t_{k+1}, \mathbf{q}_{k+1}) - \mathbf{f}_d^-(t_k, \mathbf{q}_k, t_{k+1}, \mathbf{q}_{k+1}) = \mathbf{p}_k \quad (34)$$

$$D_1 L_d(t_k, \mathbf{q}_k, t_{k+1}, \mathbf{q}_{k+1}) + g_d^-(t_k, \mathbf{q}_k, t_{k+1}, \mathbf{q}_{k+1}) = E_k \quad (35)$$

$$\mathbf{p}_{k+1} = D_4 L_d(t_k, \mathbf{q}_k, t_{k+1}, \mathbf{q}_{k+1}) + \mathbf{f}_d^+(t_k, q_k, t_{k+1}, q_{k+1}) \quad (36)$$

$$E_{k+1} = -D_3 L_d(t_k, \mathbf{q}_k, t_{k+1}, \mathbf{q}_{k+1}) - g_d^-(t_k, \mathbf{q}_k, t_{k+1}, \mathbf{q}_{k+1}) \quad (37)$$

Given a time-dependent Lagrangian system with external forcing, the extended discrete Lagrangian system obtained by solving (34)-(37) can be used as an adaptive time step variational integrator for the continuous-time system.

Remark 2. The modified discrete energy (33) has a contribution from the external forcing which accounts for the virtual work done during the adaptive time step. Thus, the discrete trajectory obtained by solving the extended discrete Euler-Lagrange equations preserves a discrete quantity which is not the discrete analogue of the total energy of the Lagrangian system. This detail becomes important when we simulate a dissipative Lagrangian system with an adaptive time step variational integrator in Section 5.3

5 Numerical Examples

In this section, we implement the extended forced discrete Euler-Lagrange equations as numerical integrators of continuous dynamical systems. We first consider a nonlinear conservative dynamical system studied in [9] and compare the fixed time step variational integrator results with the corresponding results for the adaptive time step variational integrator. We then study a forced harmonic oscillator, a time-dependent dynamical system, in order to investigate the numerical properties of the adaptive time step variational integrators for forced systems. Finally, we simulate a damped harmonic oscillator to understand the numerical performance of adaptive time step variational integrators for dissipative systems.

5.1 Conservative Example

We consider a particle in a double-well potential. The Lagrangian for this conservative one degree of freedom dynamical system is

$$L(q,\dot{q}) = \frac{1}{2}m\dot{q}^2 - V(q) \tag{38}$$

where

$$V(q) = \frac{1}{2}\left(q^4 - q^2\right) \tag{39}$$

5.1.1 Fixed time step algorithm

For the fixed time step case, we choose a constant time step h. The discrete Lagrangian is obtained using the midpoint rule

$$L_d(q_k, q_{k+1}) = hL\left(\frac{q_k + q_{k+1}}{2}, \frac{q_{k+1} - q_k}{h}\right) \tag{40}$$

The discrete momentum p_{k+1} is given by

$$p_{k+1} = m\left(\frac{q_{k+1} - q_k}{h}\right) + h\left(\left(\frac{q_{k+1} + q_k}{4}\right) - \left(\frac{q_{k+1} + q_k}{2}\right)^3\right) \tag{41}$$

For given (q_k, p_k) at the k^{th} time step, the implicit time-marching equation for the fixed time step method is

$$m\left(\frac{q_{k+1} - q_k}{h}\right) - h\left(\left(\frac{q_{k+1} + q_k}{4}\right) - \left(\frac{q_{k+1} + q_k}{2}\right)^3\right) = p_k \tag{42}$$

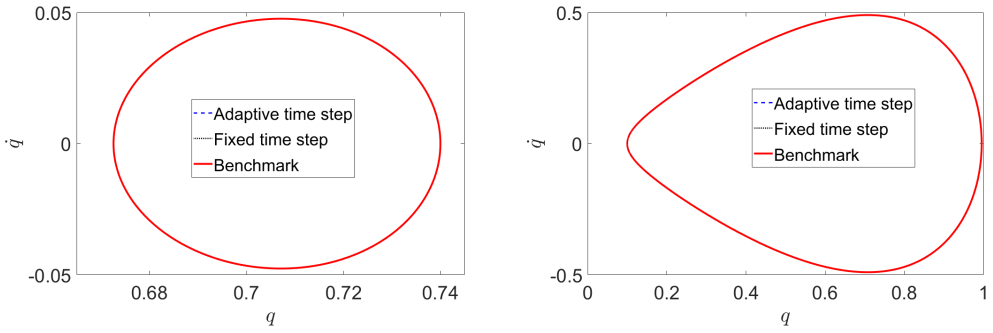

(a) $q(0) = 0.74,\ \dot{q}(0) = 0$ (b) $q(0) = 0.995,\ \dot{q}(0) = 0$

Figure 1: Two initial conditions are studied for the particle in double-well potential. An initial time step of $h_0 = 0.01$ is used for the adaptive time step algorithm in both cases. The fixed time step size is chosen such that number of total time steps is same as the adaptive algorithm. Phase space trajectories for both fixed time step and adaptive time step algorithms are compared to the benchmark trajectory. The trajectories in each figure are indistinguishable verifying the equations.

5.1.2 Adaptive time step algorithm

For the adaptive time step case, we have discrete time t_k as an additional discrete variable. We use the midpoint rule to obtain the discrete Lagrangian L_d

$$L_d(t_k, q_k, t_{k+1}, q_{k+1}) = (t_{k+1} - t_k) \left[\frac{1}{2} m \left(\frac{q_{k+1} - q_k}{t_{k+1} - t_k} \right)^2 - \frac{1}{2} \left(\left(\frac{q_{k+1} + q_k}{2} \right)^4 - \left(\frac{q_{k+1} + q_k}{2} \right)^2 \right) \right] \tag{43}$$

The discrete momentum p_k and discrete energy E_k are obtained by substituting the L_d expression in (17) and (18)

$$p_{k+1} = m \left(\frac{q_{k+1} - q_k}{t_{k+1} - t_k} \right) + (t_{k+1} - t_k) \left(\left(\frac{q_{k+1} + q_k}{4} \right) - \left(\frac{q_{k+1} + q_k}{2} \right)^3 \right) \tag{44}$$

$$E_{k+1} = \frac{1}{2} m \left(\frac{q_{k+1} - q_k}{t_{k+1} - t_k} \right)^2 + \frac{1}{2} \left(\left(\frac{q_{k+1} + q_k}{2} \right)^4 - \left(\frac{q_{k+1} + q_k}{2} \right)^2 \right) \tag{45}$$

The implicit time-marching equations for the adaptive time step algorithm are

$$m \left(\frac{q_{k+1} - q_k}{t_{k+1} - t_k} \right) - (t_{k+1} - t_k) \left(\left(\frac{q_{k+1} + q_k}{4} \right) - \left(\frac{q_{k+1} + q_k}{2} \right)^3 \right) = p_k \tag{46}$$

$$\frac{1}{2} m \left(\frac{q_{k+1} - q_k}{t_{k+1} - t_k} \right)^2 + \frac{1}{2} \left(\left(\frac{q_{k+1} + q_k}{2} \right)^4 - \left(\frac{q_{k+1} + q_k}{2} \right)^2 \right) = E_k \tag{47}$$

Since the dynamical system being considered here is time-independent, we rewrite the time-marching equations in terms of $h_k = (t_{k+1} - t_k)$ and $v_k = \left(\frac{q_{k+1} - q_k}{t_{k+1} - t_k} \right)$

$$F(q_k, p_k, h_k, v_k) = m v_k - h_k \left(\left(\frac{v_k h_k + 2 q_k}{4} \right) - \left(q_k + \frac{v_k h_k}{2} \right)^3 \right) - p_k = 0 \tag{48}$$

$$G(q_k, E_k, h_k, v_k) = \frac{1}{2} m v_k^2 + \frac{1}{2} \left(\left(q_k + \frac{v_k h_k}{2} \right)^4 - \left(q_k + \frac{v_k h_k}{2} \right)^2 \right) - E_k = 0 \tag{49}$$

These time-marching equations are solved using Newton's iterative method with the restriction $h_k > 0$ to obtain discrete trajectories in the extended space. This extended discrete system can be used as a variational integrator for the continuous-time dynamical system.

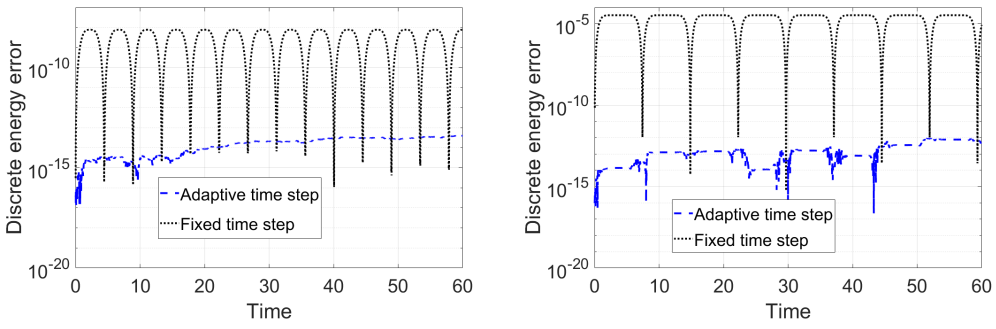

(a) $q(0) = 0.74,\ \dot{q}(0) = 0$ (b) $q(0) = 0.995,\ \dot{q}(0) = 0$

Figure 2: Energy error plots for both fixed time step and adaptive time step algorithms are compared for two different initial conditions. Each figure shows the superior energy performance of the adaptive time step algorithm.

Remark 3. In [9], an alternative optimization method has been implemented where instead of solving the nonlinear coupled equations (48) and (49), the following quantity is minimized

$$[F(q_k, p_k, h_k, v_k)]^2 + [G(q_k, E_k, h_k, v_k)]^2 \tag{50}$$

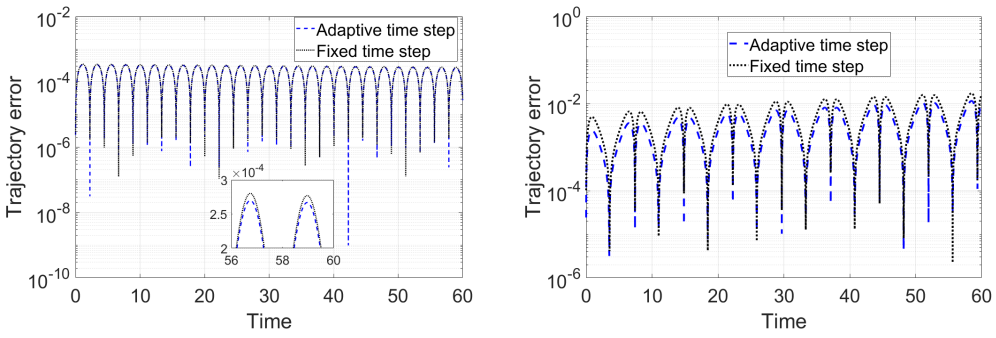

(a) $q(0) = 0.74,\ \dot{q}(0) = 0$ (b) $q(0) = 0.995,\ \dot{q}(0) = 0$

Figure 3: Trajectory error plots for both fixed time step and adaptive time step algorithms are compared for two different initial conditions. Each figure, especially the highly nonlinear case (b), clearly shows the superior trajectory performance of the adaptive time step algorithm.

over the variables v_k and h_k with the restriction $h_k > 0$. The drawback of using this approach is that numerically it violates the energy evolution equation and the underlying structure is no longer preserved. In fact, due to this optimization approach, the energy plots given in [9] do not clearly convey the advantage of energy-preserving variational integrators.

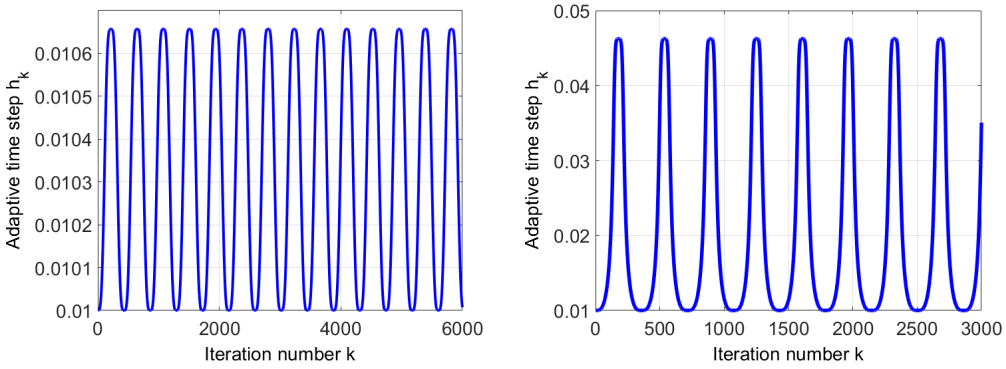

(a) $q(0) = 0.74,\ \dot{q}(0) = 0$ (b) $q(0) = 0.995,\ \dot{q}(0) = 0$

Figure 4: Adaptive time step versus iteration number for both initial conditions.

5.1.3 Initial condition

We have considered two regions of phase space, similar to the numerical example in [9], to understand numerical properties of the adaptive time step variational integrator for conservative systems. Since our aim is to use these discrete trajectories as numerical integrators for continuous dynamical systems, instead of starting with two discrete points we consider a continuous-time dynamical system with given initial position $q(0)$ and initial velocity $\dot{q}(0)$ and use the benchmark solution to obtain initial conditions for the adaptive time step variational integrator. Fixed time step determination Since the adaptive time step changes substantially from the initial time step h_0, for a fair comparison of trajectory accuracy and energy error, we have chosen the fixed time step algorithm in such a way that both fixed and adaptive algorithms take same number total time steps over the numerical simulation.

For a given set of initial conditions, i.e. $(q(0), \dot{q}(0))$, we first decide the initial time step h_0 and then use the benchmark solution to compute discrete configuration q_1 at time $t_1 = h_0$, configuration at first time step. Thus, we have obtained two discrete points in the extended state space (t_0, q_0) and (t_1, q_1) and using these two discrete points we can find discrete momentum p_1 and discrete energy E_1. After obtaining (t_1, q_1, p_1, E_1), we can solve the time-marching equations (34)-(37) to numerically simulate the dynamical system.

5.1.4 Results

The discrete trajectories for both fixed and adaptive time step algorithms are compared with the benchmark solution in Figure 1. The position $q = \frac{q_k+q_{k+1}}{2}$ and velocity $\dot{q} = \frac{q_{k+1}-q_k}{h_k}$ are computed from the discrete trajectories for both fixed and adaptive time step algorithms and compared with continuous time q and $\dot{q}$. For both initial conditions, discrete trajectories from the adaptive time step and fixed time step match the benchmark trajectory.

The energy error plots for both cases in Figure 2 show the superior energy behavior of adaptive time step variational integrators for conservative dynamical systems. Instead of using the optimization approach discussed in Remark 3, we have obtained the discrete trajectories by solving the nonlinear coupled equations exactly to preserve the underlying structure. The energy error plots quantify the difference in energy accuracy for fixed time step and adaptive time step method clearly. The energy-preserving performance was not evident in similar results given in [9] because of the optimization approach used to obtain discrete trajectories instead of solving the implicit equations directly. The energy error comparison in Figure 2a shows that the adaptive time step method has energy error magnitude around 10^{-14} whereas the fixed time step method has energy error around 10^{-8}. In Figure 2b the energy error for fixed time step increases to 10^{-6} while the adaptive time step method shows nearly exact energy preservation(of the order of computer precision minus the condition number of the equations). Although the magnitude of energy error for fixed time step method is bounded, the magnitude of energy error oscillations depends on where the trajectory lies in the phase space. Thus, for areas in phase space where the magnitude of energy error oscillations is substantial for fixed time step method, the adaptive time step method can be used to preserve the energy of the system more accurately.

Paragraph added for trajectory error plots Trajectory error plots shown in Figure 3 demonstrate the improved accuracy achieved by adaptive time step variational integrators for both cases. In Figure 3a both methods exhibit nearly same accuracy with adaptive time step performing marginally better. The trajectory error comparison in Figure 3b shows the superior performance of adaptive time step variational integrators for long time simulation. Based on the accuracy results, we believe adaptive time step variational integrators can provide benefits for numerical simulation of regions of phase space which show significant changes in the underlying physics.

Figure 4 shows how the adaptive time step oscillates for both cases. The adaptive time step doesn't increase substantially compared to the initial time step of $h_0 = 0.01$ for the first case in Figure 4a, while Figure 4b indicates the adaptive time step increases by 4 times the initial time step for the second case. The amplitude of adaptive time step oscillations depends on the region of phase space in which the discrete trajectory lies. The adaptive time step algorithm computes the adaptive time step such that the discrete energy is conserved exactly. There is no upper bound on the size of the adaptive time step, but very large adaptive time step values make the discretization assumption made in (43) erroneous leading to inaccurate discrete trajectories.

Remark 4. It is important to understand that adaptive time step variational integrators are fundamentally different from traditional adaptive time-stepping numerical methods which compute the adaptive time step size based on some error criteria. Adaptive time step variational integrators treat time as a discrete dynamic variable and the adaptive time step is computed by solving the extended discrete Euler-Lagrange equations. Thus, the adaptive time step is coupled with the dynamics of the system whereas, for most of the the adaptive time-stepping numerical methods, the step size computation and dynamics of the system are independent of each other.

5.1.5 Effect of initial time step

From the discrete energy definition it is clear that the initial time step value plays an important role in the adaptive time step algorithm. We study the effect of initial time step on the phase space and energy error plots by simulating the two cases considered in the previous subsection but with a larger initial time step $h_0 = 0.1$ for the adaptive time step. The fixed time step size is chosen such that number of total time steps is same for both fixed and adaptive time step algorithm.

The phase space trajectories shown in Figure 5 show that even with an initial time step of $h_0 = 0.1$ discrete trajectories from both fixed and adaptive time step show good agreement with the benchmark solution. In Figure 5a, the discrete trajectories lie on top of the benchmark solution for the first set of initial conditions. In Figure 5b, the fixed and adaptive time step discrete trajectories give slightly inaccurate results near the turning point. The discrete energy error

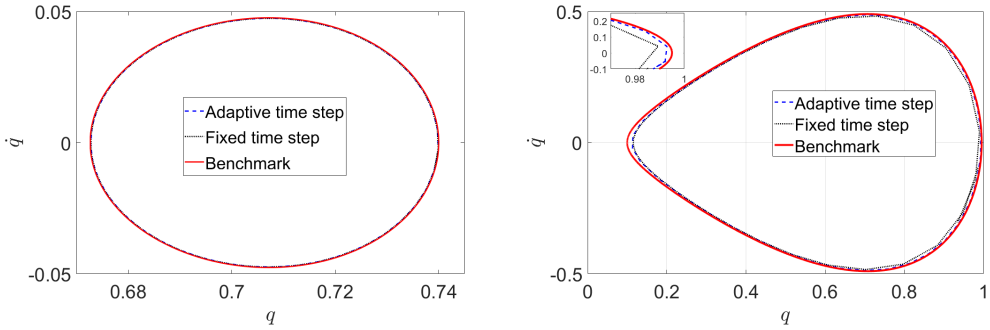

(a) $q(0) = 0.74,\ \dot{q}(0) = 0$ (b) $q(0) = 0.995,\ \dot{q}(0) = 0$

Figure 5: In these plots, an initial time step of $h_0 = 0.1$ is used for the adaptive time step algorithm to study the effect of initial time step on the accuracy of discrete trajectories.

plots in Figure 6 show that for fixed time step variational integrators, the discrete energy errors increase with increase in the time step size but for the adaptive time step variational integrators, increasing the time step size leads to accurate discrete energy behavior. In fact, the accuracy of energy preservation is slightly better for this case. This unexpected behavior is due to the ill-conditioned nature of the implicit extended discrete Euler-Lagrange equations, which become more ill-conditioned for smaller time steps. The plots of condition number in Figure 7 show that the implicit equations become more ill-conditioned as the initial time step value is decreased. Thus, numerical computations with finite precision will lead to higher errors in the solution.

It is important to note that for a conservative system, the continuous-time trajectory preserves the continuous energy which is different from the discrete energy that adaptive time step variational integrators are constructed to preserve. This explains why, despite the superior energy behavior in Figure 6b compared to Figure 2b, the discrete trajectory in Figure 5b is less accurate than the discrete trajectory in Figure 1b. We know that as the time step value tends to zero the discrete energy and continuous energy become equal but the condition number analysis and the energy error plots reveal that smaller initial time steps for adaptive time variational integrators lead to ill-conditioning and finite precision errors in energy. *Thus, there is a trade-off between preserving discrete energy and ensuring overall trajectory accuracy when choosing an initial time step for the adaptive time step variational integrators.*

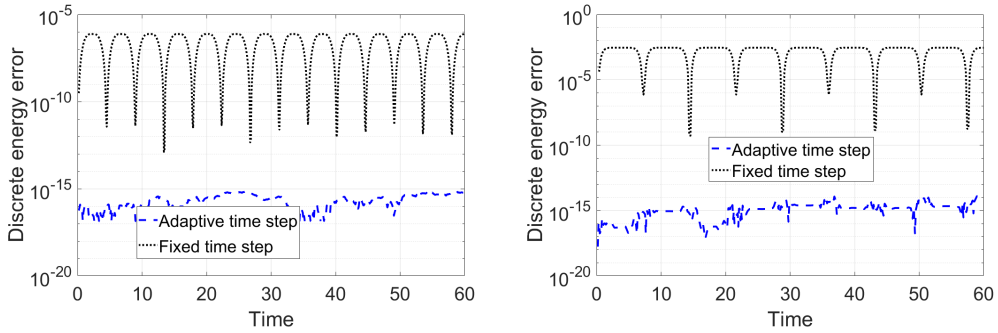

(a) $q(0) = 0.74,\ \dot{q}(0) = 0$ (b) $q(0) = 0.995,\ \dot{q}(0) = 0$

Figure 6: The energy error plots with an initial time step of $h_0 = 0.1$ for the adaptive time step algorithm.

Remark 5. The discrete energy error plotted in Figure 2 and Figure 6 is different from our traditional idea of energy error. We usually define energy error as the difference between the energy of the continuous-time system and the energy obtained from the discrete trajectories. This traditional energy error can be broken down into *discrete energy error* and *discretization error*. The discrete energy error is the error in preserving the discrete energy of the extended discrete Lagrangian system. The discretization error is the error incurred by discretizing a continuous-time system. Thus, the discretization error is the difference between the continuous energy and the

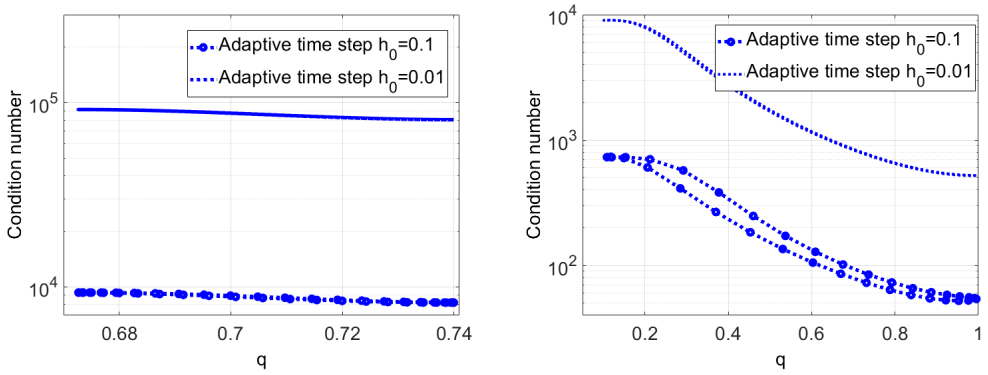

(a) $q(0) = 0.74,\ \dot{q}(0) = 0$ (b) $q(0) = 0.995,\ \dot{q}(0) = 0$

Figure 7: The increase in condition number with decrease in initial time step for the adaptive time step algorithm.

discrete energy that our integrators aim to preserve, whereas the discrete energy error is the error between the true and computed discrete energy.

Remark 6. For a conservative system, we expect discrete energy to be constant and thus the discretization error is also constant. Since this constant discretization error is orders of magnitude larger than the discrete energy error, traditional energy error plots do not show the advantages of using adaptive time-stepping. We evaluate the performance of variational integrators by comparing how well these integrators preserve the discrete energy.

5.2 Time-dependent Example

This is a new subsection We consider a forced harmonic oscillator to study the numerical performance of the adaptive time step variational integrator for forced Lagrangian systems with explicit time-dependence. The (continuous) Lagrangian for the single degree of freedom system is

$$L(q, \dot{q}) = \frac{1}{2}m\dot{q}^2 - \frac{1}{2}kq^2 \tag{51}$$

and the external forcing is

$$f = F_0 cos(\omega_F t) \tag{52}$$

where m is the mass, k is the stiffness, F_0 is the magnitude of the force and ω_F is the forcing frequency. For discretization, we use the midpoint rule to obtain the discrete Lagrangian L_d

$$L_d(t_k, q_k, t_{k+1}, q_{k+1}) = (t_{k+1} - t_k)\ L\left(\frac{q_k + q_{k+1}}{2}, \frac{q_{k+1} - q_k}{t_{k+1} - t_k}\right) \tag{53}$$

Similarly, we can write the discrete force $f_d^{\pm}$ as

$$f_d^{\pm} = \frac{1}{2}F_0(t_{k+1} - t_k)cos\left(\frac{\omega_F(t_{k+1} + t_k)}{2}\right) \tag{54}$$

and the corresponding power term $g_d^{\pm}$ as

$$g_d^{\pm} = -f_d^{\pm}\left(\frac{q_{k+1} - q_k}{t_{k+1} - t_k}\right) = -\frac{1}{2}F_0(t_{k+1} - t_k)cos\left(\frac{\omega_F(t_{k+1} + t_k)}{2}\right)\left(\frac{q_{k+1} - q_k}{t_{k+1} - t_k}\right) \tag{55}$$

The discrete momentum p_{k+1} and discrete energy E_{k+1} expressions are

$$\begin{aligned} p_{k+1} &= D_4 L_d(t_k, q_k, t_{k+1}, q_{k+1}) + f_d^+ \\ &= m\left(\frac{q_{k+1} - q_k}{t_{k+1} - t_k}\right) - k(t_{k+1} - t_k)\left(\frac{q_k + q_{k+1}}{4}\right) + \frac{F_0(t_{k+1} - t_k)}{2}cos\left(\frac{\omega_F(t_{k+1} + t_k)}{2}\right) \end{aligned} \tag{56}$$

$$\begin{aligned} E_{k+1} &= -D_3 L_d(t_k, q_k, t_{k+1}, q_{k+1}) - g_d^+ \\ &= \frac{1}{2}m\left(\frac{q_{k+1} - q_k}{t_{k+1} - t_k}\right)^2 + \frac{1}{2}k\left(\frac{q_k + q_{k+1}}{2}\right)^2 + \frac{F_0}{2}cos\left(\frac{\omega_F(t_{k+1} + t_k)}{2}\right)(q_{k+1} - q_k) \end{aligned} \tag{57}$$

For given (t_k, q_k, E_k, p_k), the time-marching implicit equations for the forced harmonic oscillator are obtained by substituting the discrete Lagrangian (53) and discrete force expressions (54)-(55) into (34) and (35)

$$m\left(\frac{q_{k+1}+q_k}{t_{k+1}-t_k}\right)+k(t_{k+1}-t_k)\left(\frac{q_{k+1}+q_k}{4}\right)+\frac{F_0(t_{k+1}-t_k)}{2}cos\left(\frac{\omega_F(t_{k+1}+t_k)}{2}\right)=p_k \quad (58)$$

$$\frac{1}{2}m\left(\frac{q_{k+1}-q_k}{t_{k+1}-t_k}\right)^2+\frac{1}{2}k\left(\frac{q_{k+1}+q_k}{2}\right)^2-\frac{F_0}{2}cos\left(\frac{\omega_F(t_{k+1}+t_k)}{2}\right)(q_{k+1}-q_k)=E_k \quad (59)$$

We re-write the above two coupled nonlinear equations in terms of the k^{th} adaptive time step $h_k = t_{k+1} - t_k$ and $v_k = \left(\frac{q_{k+1}-q_k}{t_{k+1}-t_k}\right)$

$$F(q_k, t_k, p_k, h_k, v_k) = mv_k + \frac{kh_k}{4}(2q_k + h_k v_k) + \frac{F_0 h_k}{2}cos\left(\omega_F\left(t_k+\frac{h_k}{2}\right)\right) - p_k = 0 \quad (60)$$

$$G(q_k, t_k, E_k, h_k, v_k) = \frac{1}{2}mv_k^2 + \frac{1}{2}k\left(q_k+\frac{h_k v_k}{2}\right)^2 - \frac{F_0 h_k v_k}{2}cos\left(\omega_F\left(t_k+\frac{h_k}{2}\right)\right) - E_k = 0 \quad (61)$$

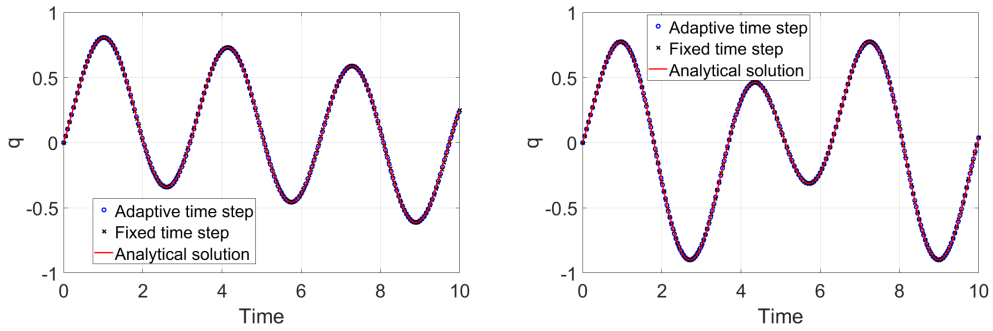

(a) $\sigma = 0.1$ (b) $\sigma = 0.5$

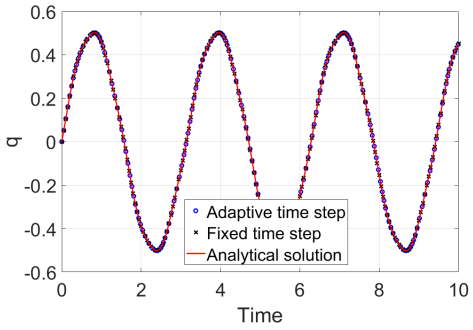

(c) $\sigma = 5$

Figure 8: Three forcing frequency ratio values are studied for the forced harmonic oscillator system. Discrete trajectories for both fixed time step and adaptive time step variational integrators are plotted and compared with the analytical solution for an initial time step $h_0 = 0.01$ for the adaptive time step algorithm and natural frequency $\omega_n = 2\ rad/s$.

5.2.1 Results

We have studied the forced harmonic oscillator for three values of the forcing frequency ratio $\sigma = \frac{\omega_F}{\omega_n}$ for $\omega_n = \sqrt{\frac{k}{m}} = 2\ rad/s$ to understand the numerical performance of adaptive time step variational integrators for systems with explicit time-dependence. The discrete trajectories from both fixed and adaptive time step variational integrators are compared in Figure 8 and both discrete trajectories agree favorably with the analytical solution for all three cases.

Energy error plots for all three cases in Figure 9 show the superior energy behavior of adaptive time step variational integrators for systems with explicit time-dependence. The energy error comparison in Figure 9a shows that the adaptive time step method has energy error magnitude around 10^{-4} whereas the fixed time step method has energy error around 10^{-2}. In Figure 9b and Figure 9c the energy error for fixed time step increases to 10^{-1} with increase in forcing frequency while the adaptive time step method still shows an energy error around 10^{-4}. Thus, adaptive time step method predict change in energy more accurately than fixed time step methods for systems with explicit time-dependence and can be used to numerically simulate nonautonomous oscillatory systems with external forcing.

The trajectory error plots in Figure 10 show how both adaptive and fixed time step integrators have similar accuracy for low forcing frequencies but, as the forcing frequency increases, the fixed time step variational integrators show better trajectory accuracy. These trajectory error results in Figure 10 are contrary to the trend of superior trajectory performance observed for conservative example in Figure 3. In Figure 10a both fixed and adaptive time step variational integrators show same trajectory error. The comparison in Figure 10b and Figure 10c show how adaptive time step variational integrators start with more accurate trajectory but, as we march forward in time, the fixed time step variational integrator exhibits lower trajectory error, especially in the case of $\sigma = 5$. This can be understood if we look at the time step adaptation.

Figure 11 shows the change in adaptive time step over the simulation time for different forcing frequencies. For all three cases, the adaptive time step starts from $h_0 = 0.01$ but oscillates significantly for higher σ. $\sigma = 0.1$ leads to a time step range of $0.0095 - 0.0105$ which increases to $0.007 - 0.022$ for $\sigma = 5$. Figure 11c shows the adaptive time step for $\sigma = 5$ quickly rise to double its initial time step $h_0 = 0.01$ and the trajectory error (see Figure 10c)also rises sharply during the increase in adaptive time step. Since the adaptive time step algorithm captures the flux of energy over an oscillation accurately , the error comes back to zero in every oscillation and hence the trajectory does deviate from the analytical trajectories in Figure 10c.

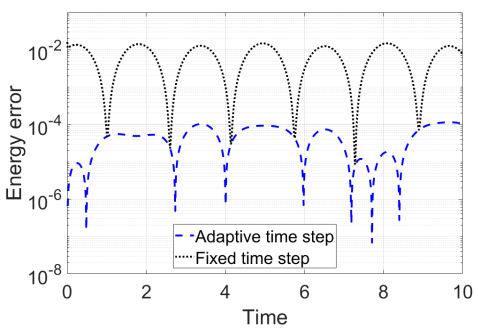

(a) $\sigma = 0.1$

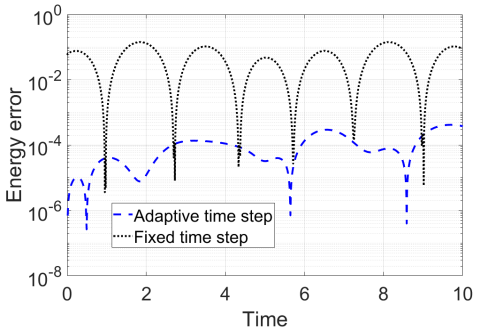

(b) $\sigma = 0.5$

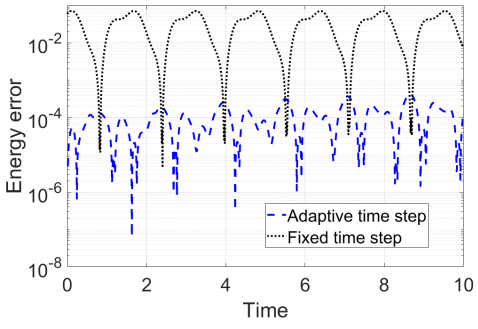

(c) $\sigma = 5$

Figure 9: Energy error for fixed time step and adaptive time step variational integrators are compared for three forcing frequencies. Analytical solution at the discrete time instant is used to compute the continuous energy.

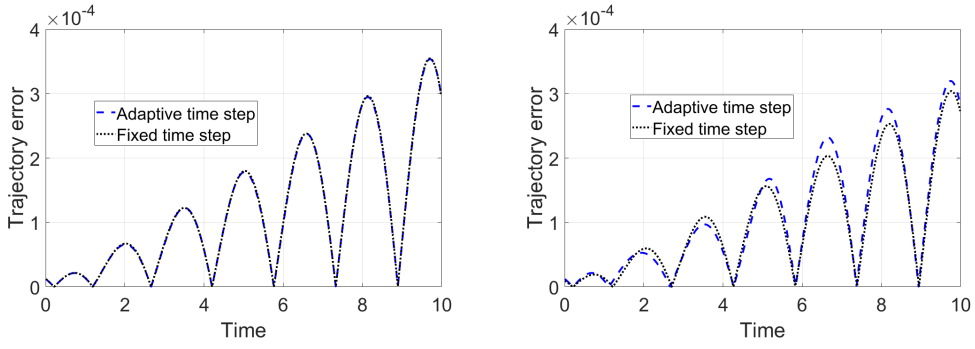

(a) $\sigma = 0.1$ (b) $\sigma = 0.5$

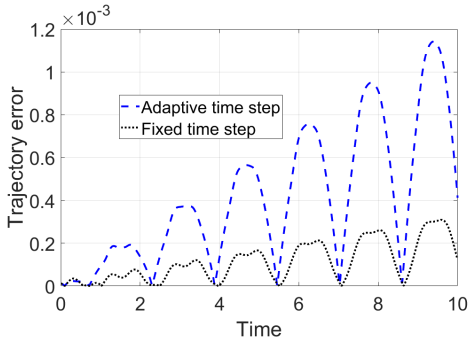

(c) $\sigma = 5$

Figure 10: Trajectory error for fixed and adaptive time step variational integrators for the forced harmonic oscillator are compared for three forcing frequency values.

5.3 Dissipative Example

We consider a damped harmonic oscillator in order to better understand the numerical behavior of the adaptive time step variational integrator for forced Lagrangian systems. Similar to the time-dependent example, the Lagrangian is given by (51) and the dissipative force is

$$f = -c\dot{q} \tag{62}$$

where c is the damping parameter of the single degree of freedom system. For the discrete Lagrangian L_d, we use the midpoint rule which gives

$$L_d(t_k, q_k, t_{k+1}, q_{k+1}) = (t_{k+1} - t_k)\, L\left(\frac{q_k + q_{k+1}}{2}, \frac{q_{k+1} - q_k}{t_{k+1} - t_k}\right) \tag{63}$$

Similarly, we can write the discrete force $f_d^{\pm}$ as

$$f_d^{\pm} = -\frac{1}{2}c(t_{k+1} - t_k)\left(\frac{q_{k+1} - q_k}{t_{k+1} - t_k}\right) \tag{64}$$

and the corresponding power term $g_d^{\pm}$ is

$$g_d^{\pm} = -f_d^{\pm}\left(\frac{q_{k+1} - q_k}{t_{k+1} - t_k}\right) = \frac{1}{2}c(t_{k+1} - t_k)\left(\frac{q_{k+1} - q_k}{t_{k+1} - t_k}\right)^2 \tag{65}$$

The discrete momentum p_{k+1} and discrete energy E_{k+1} expressions are

$$\begin{aligned} p_{k+1} &= D_4 L_d(t_k, q_k, t_{k+1}, q_{k+1}) + f_d^+ \\ &= m\left(\frac{q_{k+1} - q_k}{t_{k+1} - t_k}\right) - k(t_{k+1} - t_k)\left(\frac{q_k + q_{k+1}}{4}\right) - c\left(\frac{q_{k+1} - q_k}{2}\right) \end{aligned} \tag{66}$$

$$\begin{aligned} E_{k+1} &= -D_3 L_d(t_k, q_k, t_{k+1}, q_{k+1}) - g_d^+ \\ &= \frac{1}{2}m\left(\frac{q_{k+1} - q_k}{t_{k+1} - t_k}\right)^2 + \frac{1}{2}k\left(\frac{q_k + q_{k+1}}{2}\right)^2 - \frac{c}{2}\left(\frac{(q_{k+1} - q_k)^2}{t_{k+1} - t_k}\right) \end{aligned} \tag{67}$$

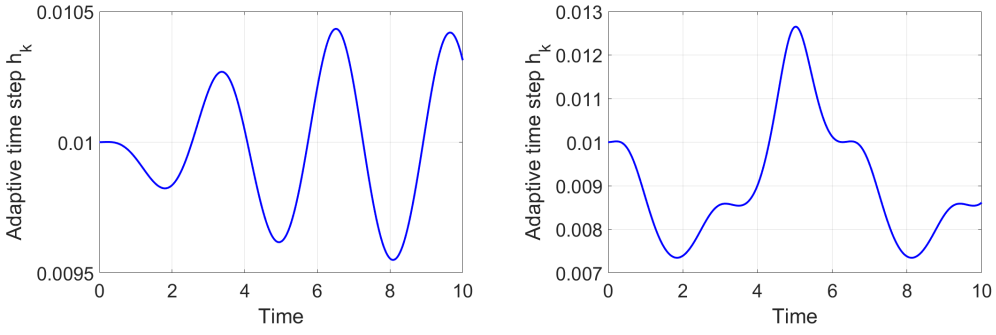

(a) $\sigma = 0.1$ (b) $\sigma = 0.5$

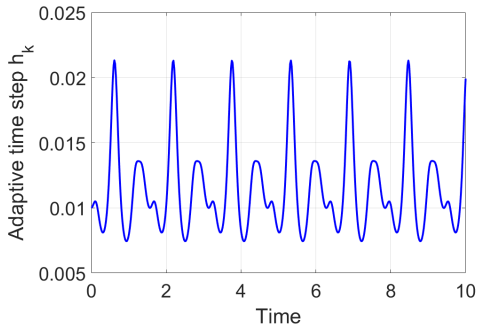

(c) $\sigma = 5$

Figure 11: Adaptive time step versus the time for the time-dependent example.

For given (t_k, q_k, E_k, p_k), the time-marching implicit equations are obtained by substituting the discrete Lagrangian and discrete force expressions into (34) and (35)

$$m\left(\frac{q_{k+1}+q_k}{t_{k+1}-t_k}\right) + k(t_{k+1}-t_k)\left(\frac{q_{k+1}+q_k}{4}\right) - c(t_{k+1}-t_k)\left(\frac{q_{k+1}-q_k}{2}\right) = p_k \tag{68}$$

$$\frac{1}{2}m\left(\frac{q_{k+1}-q_k}{t_{k+1}-t_k}\right)^2 + \frac{1}{2}c(t_{k+1}-t_k)\left(\frac{q_{k+1}-q_k}{t_{k+1}-t_k}\right)^2 + \frac{1}{2}k\left(\frac{q_{k+1}+q_k}{2}\right)^2 = E_k \tag{69}$$

The above two coupled nonlinear equations in q_{k+1} and t_{k+1} are solved with the restriction $t_{k+1} > t_k$ and substituted in (66) and (67) to obtain the discrete momentum p_{k+1} and discrete energy E_{k+1} for the next step. We re-write the above time-marching equations in terms of $h_k = t_{k+1} - t_k$ and $v_k = \left(\frac{q_{k+1}-q_k}{t_{k+1}-t_k}\right)$

$$F(q_k, p_k, h_k, v_k) = mv_k + \frac{h_k}{4}(2q_k + h_k v_k) + \frac{1}{2}ch_k v_k - p_k = 0 \tag{70}$$

$$G(q_k, E_k, h_k, v_k) = \frac{1}{2}mv_k^2 + \frac{1}{2}ch_k v_k^2 + \frac{1}{2}k\left(q_k + \frac{h_k v_k}{2}\right)^2 - E_k = 0 \tag{71}$$

Remark 7. Since the Lagrangian and the forcing for this example are both time-independent, we can simplify the implicit equations by replacing $t_{k+1} - t_k$ by the k^{th} adaptive time step h_k as shown above. For time-dependent mechanical systems with either time-dependent Lagrangian or time-dependent forcing, this simplification cannot be made and discrete time terms can not be eliminated from the implicit equations, as shown in forced harmonic oscillator numerical example in Section 5.2. Modified this comment

5.3.1 Results

We have studied the damped simple harmonic oscillator for three small damping values of the damping ratio $\zeta = \frac{c}{2\sqrt{km}}$ for a single natural frequency $\omega_n = \sqrt{\frac{k}{m}} = 2\ rad/s$ to understand the

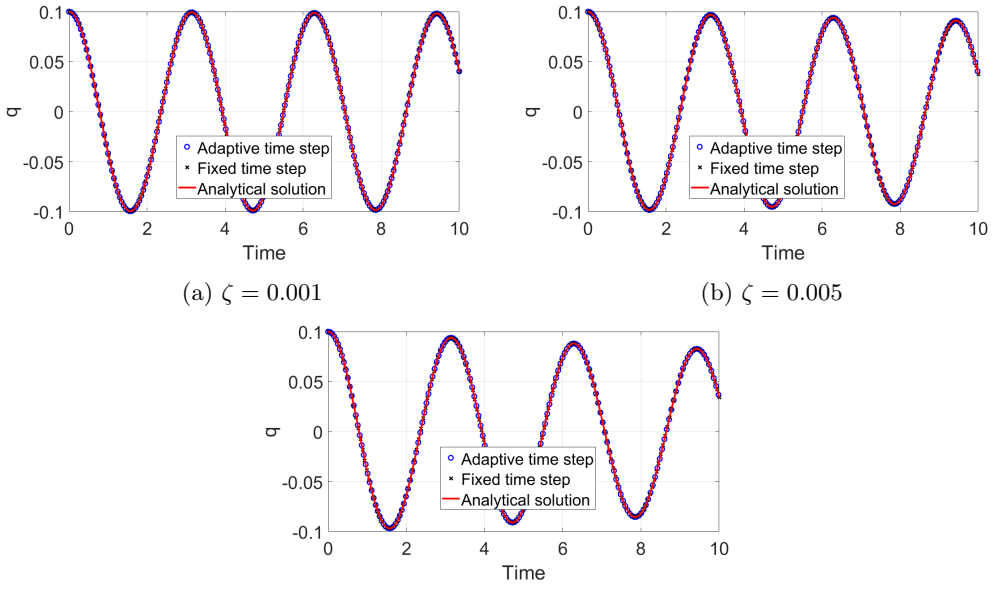

(a) $\zeta = 0.001$

(b) $\zeta = 0.005$

(c) $\zeta = 0.01$

Figure 12: Three damping ratio values are studied for the spring mass damper system. Discrete trajectories for both fixed time step and adaptive time step variational integrators are plotted and compared with the analytical solution. The analytical solution is used to prescribe initial conditions for an initial time step $h_0 = 0.01$ for the adaptive time step and natural frequency $\omega_n = 2\ rad/s$.

numerical properties of adaptive time step variational integrators derived for forced systems in Section 4. Just like the conservative case, our aim is to simulate the continuous-time dynamical system using discrete trajectories obtained from the adaptive time step variational integrator. The discrete trajectories from both fixed and adaptive time step algorithms are compared in Figure 12. Both are nearly indistinguishable from the analytical solution for all three cases.

The energy error plots in Figure 13 show how both adaptive and fixed time step variational integrators start with same energy accuracy for all three cases with adaptive time step performing better initially. As we march forward in time, the fixed time step variational integrator outperforms the adaptive time step variational integrator. *The amplitude of the energy error oscillations for the fixed time step algorithm decreases faster than it does for the adaptive time step algorithm which suggests that for long-time simulations the energy behavior of fixed time step variational integrator is better than the adaptive time step variational integrator.* This is contrary to what we expected because the adaptive step variational integrator solves an additional discrete energy evolution equation to capture the change in energy of the forced system accurately.

These unexpected results can be understood by looking at the two components of the energy error discussed in the Remark 5. Due to exact preservation of discrete energy, the discrete energy error for adaptive time step variational integrators is orders of magnitude lower than it is for the fixed time step variational integrator. Unlike the conservative system example considered in Section 5.1, the continuous energy and the corresponding discrete energy, for this dissipative system, are not constant. Thus, the energy errors are computed by comparing the continuous energy with the discrete counterpart. The discrete energy for forced Lagrangian systems has terms accounting for virtual work done by the external force during the adaptive time step and hence the adaptive time step variational integrators are preserving a discrete quantity which is not analogous to the continuous time energy. Since the difference between continuous and discrete energy is orders of magnitude larger than the discrete energy error of the variational integrator, the resulting energy error plots do not reflect the advantage of using adaptive variational integrators over fixed time step variational integrators.

Another reason behind the higher energy error for adaptive time step variational integrators is the monotonically increasing adaptive time step shown in Figure 15. The velocity approximation $\dot{q} \approx \frac{q_{k+1}-q_k}{h_k}$ used in computing the discrete energy becomes more inaccurate as the adaptive time step increases. As we go forward in time, the adaptive time step h_k keeps on increasing leading to

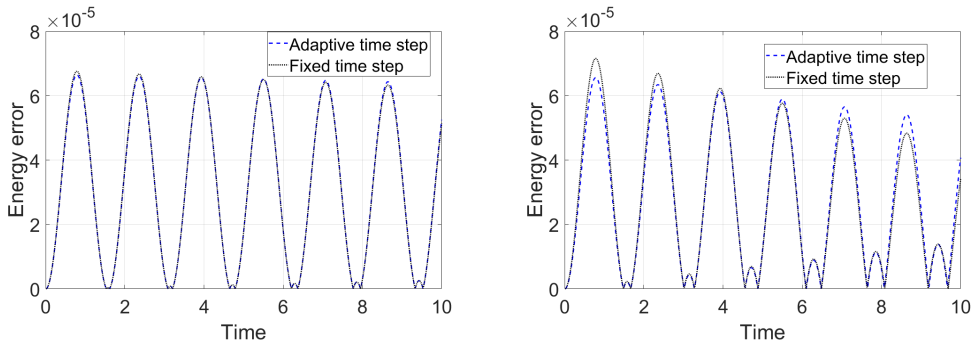

(a) $\zeta = 0.001$ (b) $\zeta = 0.005$

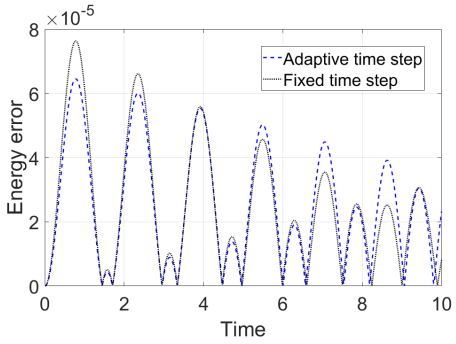

(c) $\zeta = 0.01$

Figure 13: Energy error for fixed time step and adaptive time step variational integrators are compared for three cases. Analytical solution at the discrete time instant is used to compute the continuous energy.

higher energy error for adaptive time step variational integrators. Thus, the magnitude of energy error for adaptive time does not decrease as quickly as it does for fixed time step variational integrators.

Additional paragraph to explain why adaptive time step is increasing We believe the lower order midpoint approximation used for the discrete power term in (65) is the reason behind monotonically increasing adaptive time step which leads to inaccurate energy behavior in Figure 13. The discrete power terms $g_d^{\pm}$ approximate the total work done due to time variations over an adaptive time step. Since the external forcing (62) is linearly proportional to the velocity $\dot{q}$, the integrand in (28) will be second order in $\dot{q}$. The discrete power terms $g_d^{\pm}$ in (65) approximate the integral by assuming the integrand value is constant over the adaptive time step and is equal to the value of the integrand at the midpoint $\frac{t_k+t_{k+1}}{2}$. For cases where the integrand is linear in $\dot{q}$, like in (55), the midpoint approximation works quite well yielding bounded time adaptive time steps. For the dissipative case the midpoint approximation does not capture the work done accurately resulting in increasing adaptive time step. In future, we plan to employ a higher order approximation for discrete power terms and study its effect on the adaptive time step and energy performance.

Added paragraph about trajectory accuracy plotsThe trajectory error plots for three cases in Figure 14 show the superior trajectory accuracy of adaptive time step variational integrators for dissipative systems. Due to the discretization error and changing discrete error, the increase in accuracy is not as significant as in Figure 3. The comparison in Figure 14a shows that both fixed and adaptive algorithms have almost same accuracy with adaptive method being marginally better. With increase in damping ratio, Figure 14b and Figure 14c exhibit the improved accuracy achieved by adaptive time step variational integrators. But again by the end, the accuracy of fixed time algorithm becomes similar as the adaptive time step increases.

In Figure 15 the adaptive time step evolution over time for all three damping parameter values is plotted. For all three cases, the adaptive time step was found to be monotonically increasing. This is not good for a numerical algorithm as eventually it would lead to numerical instability. We have also studied the damped harmonic oscillator system for negative damping parameter values and the results for those systems showed a uniformly decreasing adaptive time step. Thus, there

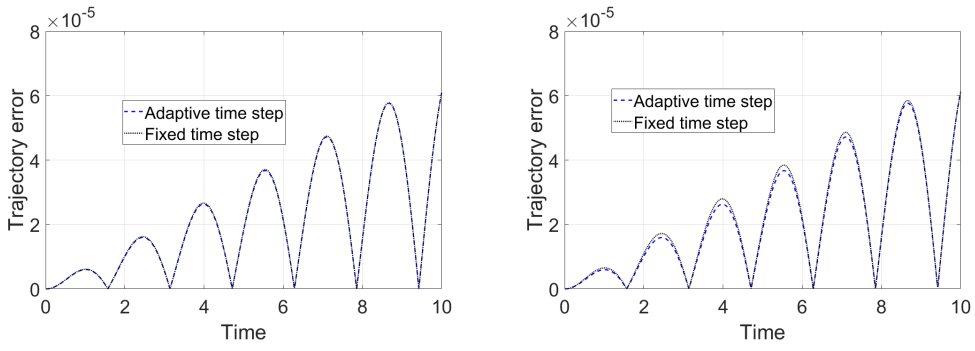

(a) $\zeta = 0.001$ (b) $\zeta = 0.005$

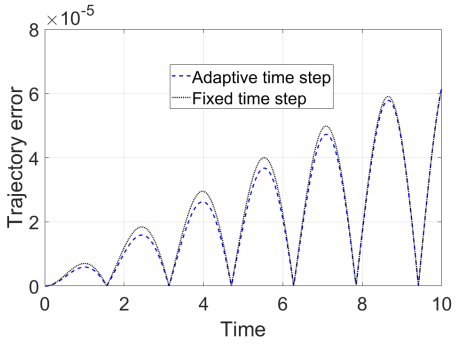

(c) $\zeta = 0.01$

Figure 14: Trajectory error for fixed and adaptive time step variational integrators for the damped harmonic oscillator are compared for three damping ratio values.

seems to be some inverse relation between the rate of change of energy and the rate of change of the adaptive time step. Again, a higher oder approximation of discrete power terms should be investigated to alleviate this adaptation.

6 Conclusions and Future work

Modified conclusions and future work In this work we have presented adaptive time step variational integrators for time-dependent mechanical systems with forcing. We have incorporated forcing into the extended discrete mechanics framework so that the resulting discrete trajectories can be used as numerical integrators for Lagrangian systems with forcing. The paper first presented the Lagrange-d'Alembert principle in the extended Lagrangian mechanics framework and then derived the extended forced discrete Euler-Lagrange equations from the discrete Lagrange-d'Alembert principle. We demonstrated a general method to construct adaptive time step variational integrators for systems with time-dependent forcing through a forced harmonic oscillator example. The results from the numerical example showed that the adaptive time step algorithm predicts the change in the energy of the nonautonomus system more accurately than the fixed time step method.

We have also presented results for a nonlinear conservative system by solving the discrete equations exactly, as opposed to the optimization approach suggested in [9]. The energy error results show the advantage of solving discrete equations exactly for adaptive time step variational integrators. We have studied the effect of initial time step on energy error and phase space trajectories and also shown how the discrete equations become more ill-conditioned as the initial time step becomes smaller.

For the damped harmonic oscillator example, contrary to expectation, the fixed time step variational integrator outperforms the adaptive time step variational integrator in energy performance. The adaptive time step for the dissipative system was found to be monotonically increasing which makes the algorithm unsuitable for long-time simulation. We believe the lower order approximation used in discrete power term is the reason behind this unexpected behavior.

In future work, we would like to study the connection between order of approximation used

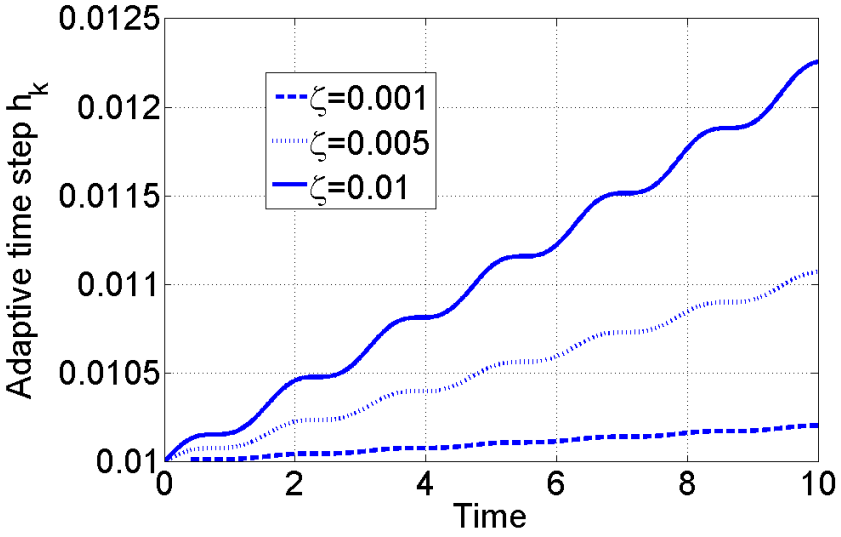

Figure 15: Adaptive time step versus the time for the dissipative example.

for discretization and the adaptive time step for the example of the damped harmonic oscillator. It would also be desirable to investigate the numerical performance of variational integrators for mechanical systems with explicitly time-dependent Lagrangian.

Acknowledgments: The authors would like to thank the anonymous reviewers for their valuable comments and suggestion to add a numerical example to improve the paper. Is this okay?

Declaration of interest: None.

Funding: This research did not receive any specific grant from funding agencies in the public, commercial, or not-for-profit sectors.

References

[1] Leimkuhler B, Reich S. Simulating Hamiltonian dynamics. Cambridge Univ. Press; 2004.

[2] Hairer E, Lubich C, Wanner G. Geometric numerical integration. 2nd ed. Berlin:Springer; 2006.

[3] Ge Z, Marsden JE. Lie-Poisson Hamilton-Jacobi theory and Lie-Poisson integrators. Phys Lett A. 1988 11;133(3):134–39.

[4] Simo JC, Tarnow N. The discrete energy-momentum method. Conserving algorithms for nonlinear elastodynamics. Z Angew Math Phys. 1992;43(5):757–92.

[5] Simo JC, Tarnow N, Wong KK. Exact energy-momentum conserving algorithms and symplectic schemes for nonlinear dynamics. Comput Methods Appl Mech Eng. 1992;100(1):63–116.

[6] Lew AJ, Mata P. A brief introduction to variational integrators. In: Structure-preserving integrators in nonlinear structural dynamics and flexible multibody dynamics. Springer; 2016. p. 201–91.

[7] Marsden JE, West M. Discrete mechanics and variational integrators. Acta Numer. 2001;10:357–514.

[8] Leok M. Generalized Galerkin variational integrators; 2005. arXiv:math/0508360 [math.NA].

[9] Kane C, Marsden JE, Ortiz M. Symplectic-energy-momentum preserving variational integrators. J Math Phys. 1999;40(7):3353–71.

[10] Shibberu Y. Discrete-time Hamiltonian dynamics [Ph.D.thesis]; U. of Texas at Arlington. 1992.

[11] Shibberu Y. Is symplectic-energy-momentum integration well-posed?; 2006. arXiv:math-ph/0608016.

[12] Shibberu Y. How to regularize a symplectic-energy-momentum integrator; 2005. arXiv:math/0507483 [math.NA].

[13] Marsden JE, Pekarsky S, Shkoller S, West M. Variational methods, multisymplectic geometry and continuum mechanics. J Geom Phys. 2001;38(3):253–84.

[14] Goldstein H. Classical Mechanics. Reading, MA: Addison-Wesley; 1980. 672 pages.